Physics and Imaging in Radiation Oncology 14 (2020) 53–60

Contents lists available at ScienceDirect

Physics and Imaging in Radiation Oncology

journal homepage: www.elsevier.com/locate/phro

Dose accumulation to assess the validity of treatment plans with reduced margins in radiotherapy of head and neck cancer

Nicholas J. Lowther[a,b], Steven H. Marsh[b], Robert J.W. Louwe[a,*]

[a] Wellington Blood and Cancer Centre, Department of Radiation Oncology, Wellington, New Zealand
[b] University of Canterbury, School of Physical and Chemical Sciences, Christchurch, New Zealand

ARTICLE INFO

Keywords:
Head-and-neck radiotherapy
DIR dose accumulation
PTV margin reduction
Plan robustness
Anatomical changes

ABSTRACT

Background and purpose: Literature has reported reduced treatment toxicity in head-and-neck radiotherapy (HNRT) when reducing the planning target volume (PTV) margin from 5 to 3 mm but loco-regional control was not always preserved. This study used deformable image registration (DIR)-facilitated dose accumulation to assess clinical target volume (CTV) coverage in the presence of anatomical changes.
Materials and methods: VMAT plans for 12 patients were optimized using 3 or 5 mm PTV and planning risk volume (PRV) margins. The planning computed tomography (*pCT*) scan was registered to each daily cone beam CT (CBCT) using DIR. The inverse registration was used to reconstruct and accumulate dose (D^{acc}). CTV coverage was assessed using the dose-volume histogram (DVH) metric $D_{99\%}^{acc}$ and by individual voxel analysis. Both approaches included an uncertainty estimate using the 95% level of confidence.
Results: $D_{99\%}^{acc}$ was less than 95% of the prescribed dose D^{presc} for three cases including only one case where this was at the 95% level of confidence. However for many patients, the accumulated dose included a substantial volume of voxels receiving less than 95% D^{presc} independent of margin expansion, which predominantly occurred in the subdermal region. Loss in target coverage was very patient specific but tightness of target volume coverage at planning was a common factor leading to underdosage.
Conclusion: This study agrees with previous literature that PTV/PRV margin reduction did not significantly reduce CTV coverage during treatment, but also highlighted that tight coverage of target volumes at planning increases the risk of clinically unacceptable dose delivery. Patient-specific verification of dose delivery to assess the dose delivered to each voxel is recommended.

1. Introduction

The introduction of intensity modulated radiotherapy has enabled highly conformal dose deliveries which allow dose reduction to organs at risk (OARs), and result in reduced treatment toxicity [1–3]. These highly conformal treatments require image-guided radiotherapy (IGRT) to warrant accurate patient positioning and monitoring of changes in patient anatomy [4]. Planning target volume (PTV) margins are applied to target volumes [5] during treatment planning to account for uncertainties such as patient positioning, geometrical accuracy of the treatment machine and geometrical uncertainties of target volume definition. The presence of these uncertainties have also prompted a recommendation to apply a planning risk volume (PRV) margin to critical OARs [6]. PTV and PRV margins of 5 mm are commonly applied in head-and-neck radiotherapy (HNRT) [7–9]. However, PTV margin recipes [10,11] do not account for non-rigid anatomy changes (i.e., changes in patient pose, weight loss, tumor response, OAR shift and shrinkage) which are commonly observed in HNRT [12–14]. Nevertheless, two groups have reported favorable toxicity profiles while maintaining good two-year loco-regional (LR) control rates after reducing the PTV margin from 5 to 3 mm [15–17]. More recently, a third study by Franzese et al. [18] reported a significant difference in the two-year LR control rates between patients treated with 5 or 3 mm PTV margins. In the latter study, a 3 mm PTV margin was associated with a decreased rate of LR control. A retrospective study by van Kranen et al. [19] found a slight increase in the risk of clinical target volume (CTV) underdosage when reducing the PTV margin from 5 to 3 mm while a similar study by Wu et al [20] concluded that the coverage of the CTVs at the end of treatment was not affected by a PTV margin reduction. Considering these differing results, further investigation of risk factors that could jeopardize a patient's CTV coverage and/or critical OAR avoidance in a reduced margin setting is warranted.

* Corresponding author.
E-mail address: rob.louwe@ccdhb.org.nz (R.J.W. Louwe).

https://doi.org/10.1016/j.phro.2020.05.004
Received 27 February 2020; Received in revised form 25 April 2020; Accepted 15 May 2020

Table 1
Structure-specific average and range for the planned, accumulated and Δ doses. HD = high-dose. ID = intermediate-dose. LD = low-dose. CTV = clinical target volume. PTV = planning target volume. SC = spinal cord. BS = brainstem. PRV = planning risk volume. PG = parotid gland. SMG = submandibular gland. Ips. = ipsilateral. Contra. = contralateral. D^{plan} = planned dose. D^{acc} = accumulated dose. ΔD = change in dose = D^{acc} - D^{plan}. $D_{99\%}$ = dose to 99% of volume. $D_{98\%}$ = dose to 98% of volume. $D_{0.1cc}$ = minimum dose to 0.1 cm^3 of the volume receiving the highest dose. D_{mean} = mean dose. ψ = number of cases where ΔD was outside the 95% level of confidence. δ = number of cases where $D^{acc}_{99\%}$ was less than 95% of the prescribed dose at the 95% level of confidence. *Indicates a statistically significant difference.

				D^{plan} [Gy]			D^{acc} [Gy]			ΔD [Gy]				
Metric	Structure	n	PTV/PRV expansion	Median	Range	p-value	Median	Range	p-value	Median	Range	p-value	ψ	δ
$D_{99\%}$	HD-CTV	11	3 mm	65.1	63.6–65.7	0.66	65.0	62.7–65.9	0.24	−0.3	−1.7 to 0.6	0.04*	9	1
			5 mm	65.0	63.7–65.9		65.4	62.0–66.3		0.3	−2.2 to 0.7		10	0
	ID-CTV	4	3 mm	60.1	59.0–60.4	0.91	60.2	58.9–60.4	0.37	0.1	−0.3 to 0.2	0.44	3	0
			5 mm	60.0	59.6–60.2		60.2	59.8–60.6		0.4	−0.4 to 0.6		4	0
	LD-CTV	12	3 mm	53.5	52.3–54.1	0.08	53.3	52.0–54.4	< 0.01*	−0.1	−1.0 to 0.3	0.01*	9	0
			5 mm	53.7	52.5–54.6		54.1	52.4–55.1		0.2	−0.8 to 0.6		10	0
$D_{98\%}$	HD-PTV	11	3 mm	63.5	62.7–64.2	0.23	62.0	59.8–63.3	0.66	−1.4	−3.1 to −0.4	0.08	11	
			5 mm	63.4	62.8–63.6		62.5	59.8–63.2		−0.9	−3.0 to −0.3		11	
	ID-PTV	4	3 mm	57.6	57.1–58.2	0.53	56.3	55.5–56.8	0.12	−1.4	−1.8 to −0.9	0.03*	4	
			5 mm	57.6	57.2–57.7		56.7	56.3–56.9		−0.8	−1.2 to −0.7		4	
	LD-PTV	12	3 mm	51.7	51.3–53.4	0.11	50.2	49.0–52.0	0.05*	−1.5	−2.9 to −0.5	0.14	12	
			5 mm	52.0	51.4–53.5		50.6	50.0–52.0		−1.3	−2.2 to −0.7		12	
$D_{0.1cc}$	SC	12	3 mm	34.1	19.4–43.4	0.63	34.5	19.9–42.5	0.54	−0.1	−1.0 to 1.0	0.33	6	
			5 mm	36.0	23.5–42.3		36.1	24.1–41.8		0.1	−0.8 to 1.2		3	
	BS	12	3 mm	37.1	30.0–51.9	0.63	37.7	30.1–51.5	0.58	0.2	−2.1 to 1.7	0.41	5	
			5 mm	35.6	27.1–52.4		35.4	26.5–52.3		0.1	−1.4 to 1.1		2	
$D_{0.1cc}$	SC PRV	12	3 mm	38.7	21.1–45.2	0.03*	38.7	21.4–43.9	0.04*	−0.7	−1.6 to 1.0	0.83	10	
			5 mm	42.1	26.6–47.4		41.3	26.7–47.9		−0.3	−2.7 to 0.5		7	
	BS PRV	12	3 mm	41.5	33.7–52.9	0.02*	41.3	32.6–52.7	< 0.01*	0.3	−1.1 to 2.3	0.60	2	
			5 mm	45.3	36.5–60.7		45.5	35.8–61.1		−0.4	−0.9 to 2.6		1	
D_{mean}	Ips. PG	14	3 mm	28.0	14.1–43.6	< 0.01*	28.8	14.1–43.0	< 0.01*	0.4	−0.7 to 2.1	0.57	5	
			5 mm	31.9	16.8–50.0		33.4	16.7–49.4		0.4	−0.6 to 2.1		5	
	Contra. PG	10	3 mm	17.1	4.5–32.8	< 0.01*	17.9	4.6–32.2	< 0.01*	0.1	−0.6 to 1.2	0.71	7	
			5 mm	21.8	5.2–37.2		22.7	5.3–36.7		0.2	−0.9 to 1.3		6	
D_{mean}	Ips. SMG	13	3 mm	63.5	1.1–65.8	0.01	62.8	1.2–66.0	< 0.01*	0.0	−1.7 to 0.7	0.17	6	
			5 mm	64.1	1.5–66.1		64.0	1.6–66.2		0.1	−1.8 to 0.7		7	
	Contra. SMG	9	3 mm	50.7	0.7–55.5	0.04*	50.5	0.7–55.9	0.03*	0.0	−1.1 to 1.3	0.74	6	
			5 mm	51.3	0.9–56.0		50.8	0.9–56.2		0.0	−0.7 to 0.8		6	

This study utilized deformable image registration (DIR) facilitated dose accumulation to objectively assess the adequacy of target coverage, critical OAR avoidance and non-critical OAR sparing when either 5 or 3 mm PTV and PRV margins were applied. In addition, the occurrence, location and trends where CTV coverage and critical OAR avoidance could be at risk was investigated. This study contributes to the scarce body of literature regarding the robustness of treatment plans for anatomical changes during HNRT when margins are reduced. While used retrospectively in this study, the presented dose accumulation analysis is primarily intended for prospective clinical application.

2. Materials and methods

2.1. Treatment immobilization, planning and on-treatment imaging

Twelve patients with cancers in the head-and-neck region that were previously treated radically were selected for this study. The patients' characteristics are summarized in Supplementary Material A. The planning computed tomography (*pCT*) scans (Brilliance Big Bore; Philips Medical Systems, Eindhoven, The Netherlands) had a voxel size of 1.3 × 1.3 × 3.0 mm^3. Patients were immobilized using a 2.4 mm Reloadable Head and Shoulder S-Frame Kevlar Mask (Q-Fix, Avondale PA, USA) and an individual head and shoulder support vacuum bag (Klarity Medical Products, Newark OH, USA).

Each patient's *pCT* was used to generate two volumetric modulated arc therapy (VMAT) plans (Eclipse Treatment Planning, Varian Medical Systems, Palo Alto CA, USA) using either 5 or 3 mm PTV and PRV margin expansions from the CTVs and critical OARs (i.e., brainstem and spinal cord), respectively. Plan optimization was carried out using the protocol in Supplementary Material B, using a dose calculation grid size of 2.5 × 2.5 × 3.0 mm^3. For eleven patients, a 5 mm expansion of the gross tumor volume (GTV) was used to generate the high-risk CTV with a prescribed dose of 66 Gy in all but one case where a compartmentalization approach [21] was used. For one patient with a benign tumor, the prescribed dose to the target volume was 54 Gy and the CTV was created by a 3 mm expansion of the GTV (see Supplementary Material A and C). For four patients, an intermediate-risk CTV was defined with a prescribed dose of 60 Gy to include anatomical structures with a high probability of infiltration based on positron-emission tomography (PET) imaging and experience of the radiation oncologist. The low-risk CTV included structures as per intergroup consensus guidelines [22] and was planned to 54 Gy. All plans used two full arcs to create a highly conformal dose distribution around the 54 Gy low-risk CTV and simultaneous integrated boost volumes to 60 and 66 Gy in 30 fractions. To achieve similar plans in terms of conformity and avoid a bias in the plan comparison, the first author (NL) generated each patient's 3 and 5 mm plan in immediate succession. All plans fulfilled the departmental criteria for treatment plan acceptance which are based on the studies of Doornaert et al. [23] and Verbakel et al. [24] and adhere to ICRU guidelines [25]. Plans were reviewed by a senior clinician involved in HNRT and a senior medical physicist who deemed the plans clinically acceptable. In a small number of cases where a CTV was located superficially within 3 mm of the external contour without the use of bolus, that CTV was cropped 3 mm from the external contour for plan evaluation and dose accumulation analysis with "virtual bolus" being applied during plan optimization to moderate the fluence in the skin region [26]. In those cases, the treating radiation oncologist omitted the use of bolus to reduce the risk of severe skin toxicity. PTVs that were located within 3 mm of the external contour were cropped back 3 mm from the skin for plan evaluation after optimization.

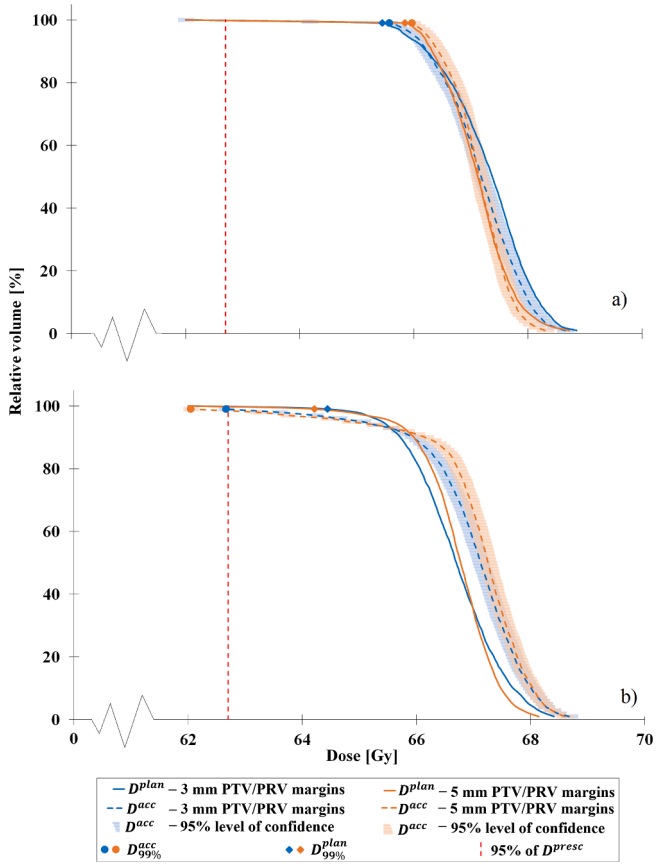

Fig. 1. Dose-volume histograms (DVHs) of $D^{plan}$and D^{acc} for the high-dose clinical target volume (CTV) of patient 8 (a) and patient 10 (b). In contrast to (a), a CTV underdosage is observed for case (b) when utilizing 3 and 5 mm planning target volume (PTV) margin plans at the 95% level of confidence (b). D^{plan} = planned dose. D^{acc} = accumulated dose. $D_{99\%}$ = dose to 99% of volume. D^{presc} = prescribed dose.

Daily (n = 30) cone beam computed tomography (CBCT) scans were acquired to verify patients' treatment position. The CBCT scans with a voxel size of 0.5 × 0.5 × 2 mm^3 were acquired prior to treatment using a Varian Truebeam (v2.0 or v2.5; Varian Medical Systems, Palo Alto CA, USA). For a minority of treatment fractions, CBCT scans were acquired on a Varian Clinac (v2.1) with a voxel size of 0.7 × 0.7 × 2.5 mm^3. All patients consented to their data being used for retrospective audits which conforms to the guidelines of the local ethics committee.

2.2. Dose accumulation and uncertainty estimation

The total delivered dose at each successive fraction was calculated according to the DIR-facilitated dose accumulation workflow previously described [27]. In summary, first a 6 degree of freedom rigid bony anatomy registration of the CBCT and the *pCT* was performed. Second, the *pCT* was deformed to match the anatomy of each daily CBCT using Varian's demons DIR implementation in SmartAdapt (SA) (v.13.6, Varian Medical Systems, Palo Alto CA, USA), which produced a deformed *pCT* (*dCT*) and a 'forward' deformation vector field (DVF). Third, the original treatment plan was recalculated on the *dCT* using the beam arrangement, monitor units and fluence maps from the original treatment plan. The resulting dose distribution was mapped back to the *pCT* space according to the true inverse DVF, producing the fraction-specific reconstructed dose. Fourth, the reconstructed dose distributions of successive fractions were accumulated. The true inverse DVF calculation and dose accumulation of the individual fraction reconstructed doses was carried out using 3D Slicer (v4.8) which is available as freeware [28,29].

The uncertainty in the dose accumulation procedure was assessed in a previous study [27] by comparing DIR-facilitated dose accumulation using SA with the results of an *in silico* model based on clinically observed deformations as ground truth. These differences were separately calculated for inverse consistent and inverse *in*consistent voxels. The distinction between those voxels was made by successive application of the forward DVF and inverse DVF and classifying the net shifts larger than one dose calculation voxel as inverse *in*consistent. These results from the previous study were subsequently used in the current study to calculate the dose reconstruction uncertainties of inverse consistent u_c and inverse *in*consistent u_i voxels. The 95% level of confidence of the accumulated dose for a single voxel within structure S at fraction f, uA_f^S is:

$$uA_f^{S+}[\%] = \frac{\sqrt{\sum_{i=1}^{f}(D_i^r . u)^2}}{D_f^a} \times 100\% u = \begin{cases} u_c^{S+} if \;\; inverse \;\; consistent \\ u_i^{S+} if \;\; inverse \;\; inconsistent \end{cases} \quad (1a)$$

$$uA_f^{S-}[\%] = \frac{\sqrt{\sum_{i=1}^{f}(D_i^r . u)^2}}{D_f^a} \times 100\% u = \begin{cases} u_c^{S-} if \;\; inverse \;\; consistent \\ u_i^{S-} if \;\; inverse \;\; inconsistent \end{cases} \quad (1b)$$

where D_i^r are the reconstructed doses of each fraction and D_f^a is the accumulated dose for fraction f. The 95% level of confidence for each dose bin in the (cumulative) DVH of the accumulated dose was calculated by averaging uA_f of all voxels with D_f^a equal to or larger than that dose level.

2.3. Dose analysis

The accumulated dose at the end of treatment, $D^{acc}$was analyzed for target volumes and OARs as detailed in Supplementary Material C for both 5 and 3 mm margin expansion plans. The difference between the planned dose D^{plan} and D^{acc} was defined as the change in dose, ΔD. From this point onward, DVH dose metrics of D^{plan}, D^{acc} and ΔD will be expressed using subscripts. For example, $D^{acc}_{99\%}$ refers to the minimum accumulated dose delivered to 99% of the volume. Target coverage of the PTV was assessed using $D_{98\%}$ to be consistent with both our department protocol and existing literature [25,30]. The CTV coverage was quantified using $D_{99\%}$ to enable direct comparison of our results with those reported by van Kranen et al. [19]. However, DVH metrics inherently lack spatial information regarding the dose distribution within a volume of interest [31] and specifically for large target volumes, a clinically relevant loss in sub-volume coverage may not be detected. Therefore, CTV coverage was also assessed by recording the number of voxels where D^{plan} and D^{acc} were less than 95% of D^{presc} at the 95% level of confidence. In addition, a more in-depth investigation was conducted to quantitatively assess coverage near the skin considering that target coverage was often already tight during treatment planning in this region. Specifically, the dependence of target coverage both during planning and treatment on the minimum distance between the CTV and skin was investigated. For that purpose, *local* volumes of approximately 0.5 cm^3 were defined at the point of minimum distance between the high-dose (HD) CTV and skin. A detailed methodology how the *local* volumes were constructed is provided in Supplementary Material D.

2.4. Statistical analyses

The normality of the distributions of the DVH parameters D^{plan}, D^{acc} and the difference ΔD between these metrics for the two margin expansions' structures were tested using Q-Q plots and Shapiro-Wilk tests as detailed in Supplementary Material E. Unless stated otherwise, two-

Table 2
Target coverage for individual patients' high-dose (HD) and intermediate-dose (ID) clinical target volume (CTV). D^{plan} = planned dose. D^{acc} = accumulated dose. D^{presc} = prescribed dose. $D_{99\%}$ = minimum dose received by 99% of volume.

CTV	Patient	Volume [cm^3]†	Margin expansion	N_{voxels} < 95% D^{presc}		$D_{99\%}$ [Gy] (95% level of confidence)	
				D^{plan}	D^{acc}	D^{plan}	D^{acc}
HD-CTV 95% D^{presc} = 62.7 Gy	1	88.0	3 mm		6*	64.8	64.5 (−0.13; +0.15)
			5 mm	15*	17*	64.3	64.1 (−0.13; +0.15)
	3	57.1	3 mm		4*	64.7	65.3 (−0.13; +0.15)
			5 mm			65.0	65.7 (−0.13; +0.15)
	4	43.6	3 mm			65.2	64.8 (−0.13; +0.15)
			5 mm			65.2	65.6 (−0.13; +0.15)
	5	56.1	3 mm			65.1	65.5 (−0.13; +0.15)
			5 mm			65.1	65.7 (−0.13; +0.15)
	6	42.4	3 mm			65.7	65.3 (−0.13; +0.15)
			5 mm			65.1	65.4 (−0.13; +0.15)
	7	112.4	3 mm		58*	64.6	63.9 (−0.13; +0.15)
			5 mm		36*	64.6	64.9 (−0.13; +0.15)
	8	46.4	3 mm			65.4	65.6 (−0.13; +0.15)
			5 mm			65.8	66.0 (−0.13; +0.15)
	9	88.5	3 mm			65.5	65.9 (−0.13; +0.16)
			5 mm			64.6	65.1 (−0.13; +0.15)
	10	57.2	3 mm	19*	127*	64.4	62.7 (−0.13; +0.15)$^\pm$
			5 mm	35*	175*	64.2	62.0 (−0.13; +0.15)*
	11	219.3	3 mm	71*	77*	65.2	65.0 (−0.13; +0.15)
			5 mm	12*	27*	65.9	66.3 (−0.14; +0.16)
	12	66.1	3 mm	58*	99*	63.6	62.8 (−0.13; +0.15)$^\pm$
			5 mm	37*	86*	63.7	63.0 (−0.13; +0.15)
ID-CTV 95% D^{presc} = 57.0 Gy	6	78.3	3 mm		4*	60.0	60.3 (−0.16; +0.11)
			5 mm			59.6	60.0 (−0.16; +0.11)
	9	211.3	3 mm	4*	9*	60.2	60.4 (−0.16; +0.11)
			5 mm			60.0	60.4 (−0.16; +0.11)
	10	171.1	3 mm		13*	60.4	60.1 (−0.16; +0.11)
			5 mm		2*	60.0	60.6 (−0.16; +0.11)
	12	113.8	3 mm	4*	13*	59.0	58.9 (−0.16; +0.11)
			5 mm		2*	60.2	59.8 (−0.16; +0.11)

†1 cm^3 includes 189 voxels.
*Dose less than 95% D^{presc} at the 95% level of confidence.
$^\pm$ Dose less than 95% D^{presc} but not at the 95% level of confidence.

tailed paired Student's t-tests at a 5% level of significance were conducted for normally distributed metrics. The number of cases where ΔD was outside the 95% level of confidence, i.e., when the 95% CI of D^{acc} did not include D^{plan}, was defined as ψ. The number of cases where a CTV $D^{acc}_{99\%}$ was less than 95% of D^{presc} at the 95% level of confidence was defined as δ.

3. Results

3.1. Target volumes

No significant difference was observed between the coverage of target volumes for the two margin expansions at planning (Table 1) due to the minimum requirement for $D^{plan}_{98\%}$ of the PTVs in the applied planning protocol (Supplementary Material B). There was also no significant difference between the observed D^{acc} during treatment for the two margin expansions, except for the low-dose (LD) target volumes LD-CTV and LD-PTV (Table 1). The average loss in target volume coverage during treatment relative to D^{plan}, ΔD, over all patients was significantly different between 5 and 3 mm margin expansions for the HD-CTV ($p = 0.04$), LD-CTV ($p = 0.01$) and intermediate-dose (ID) PTV ($p = 0.03$), although these differences were small. Example cases where the HD-CTV coverage during treatment was either well preserved or not are presented in Fig. 1a and b, respectively. A loss in coverage at the 95% level of confidence (i.e., ψ) was observed for at least 75% of all CTVs. However for only three cases, $D^{acc}_{99\%}$ was less than 95% of the prescribed dose D^{presc}. For only one case (i.e., δ), this dose difference was at the 95% level of confidence.

Table 2 further details the number of voxels with less than 95% of D^{presc} for the HD-CTVs and ID-CTVs in conjunction with the observed CTV $D_{99\%}$ for individual patients. It shows that for a majority of patients, either one or both margin expansion plans included voxels that received less than 95% D^{presc} during treatment, and that this already occurred during treatment planning for many cases. In four patients, the voxels in the HD-CTV that received less than 95% D^{presc} at the 95% confidence level were located in the subdermal region (Patients 1, 10–12). For these cases, both the PTV and the CTV were not fully covered by the 95% isodose at planning except for one case (patient one; 3 mm plan) where the CTV was covered at planning. For patient three, progressive anatomical changes during treatment resulted in a small number of voxels ($n = 4$) at the superior side of an involved node (level 2a) receiving less than 95% D^{presc}. For patient seven, voxels in the HD-CTV receiving less than 95% D^{presc} were located in the posterior soft palate where target volume coverage was already tight during planning (95% D^{presc} isodose situated midway between the PTV and CTV). For the ID-CTV, voxels receiving less than 95% D^{presc} for patients nine, ten and twelve were located in the subdermal region. For patient six, this underdosage was present at the left posterior aspect of the mandible where target volume coverage was tight during planning as well.

Further investigation of the relation between target coverage at the end of treatment and coverage at treatment planning showed that there was no obvious correlation between the HD-CTV $D^{acc}_{99\%}$and the HD-PTV $D^{plan}_{98\%}$ (Fig. 2a). There appeared to be a correlation between the HD-CTV $D^{acc}_{99\%}$ and HD-CTV $D^{plan}_{99\%}$ which were approximately equal for cases where $D^{plan}_{99\%}$ was larger than 98% D^{presc} (Fig. 2b). For the two patients where $D^{plan}_{99\%}$ was smaller than 98% D^{presc}, both margin expansion plans exhibited a larger drop in coverage during treatment in the superficial region. There was no obvious correlation between the planned and received dose for individual voxels (Fig. 3). This was further illustrated

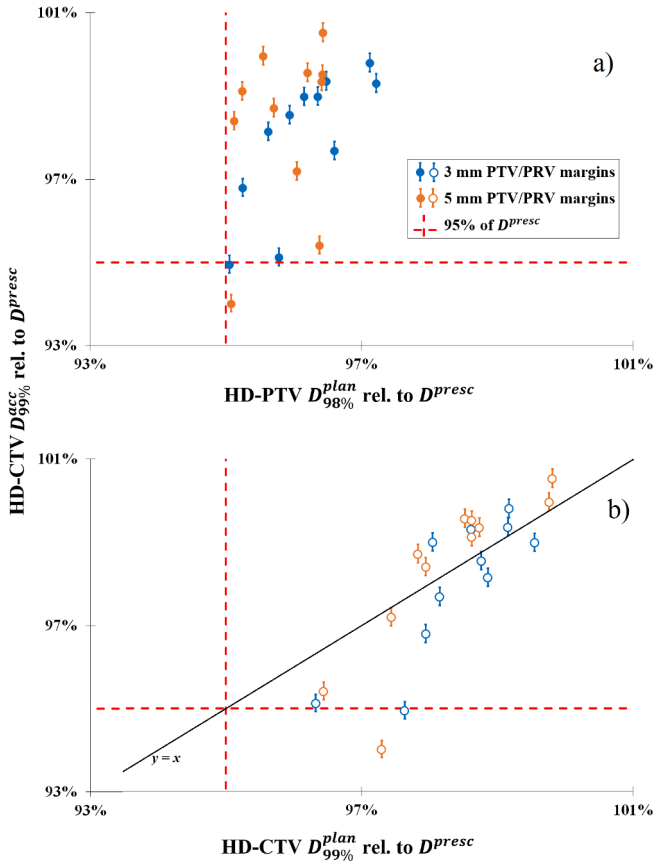

Fig. 2. Plots of dose-volume histograms (DVH) metrics of interest for the high-dose (HD) clinical target volume (CTV) and planning target volume (PTV) when utilizing 3 or 5 mm planning target volume (PTV) and planning risk volume (PRV) margin plans. D^{plan} = planned dose. D^{acc} = accumulated dose. D99% = dose to 99% of volume. D98% = dose to 98% of volume. D^{presc} = prescribed dose.

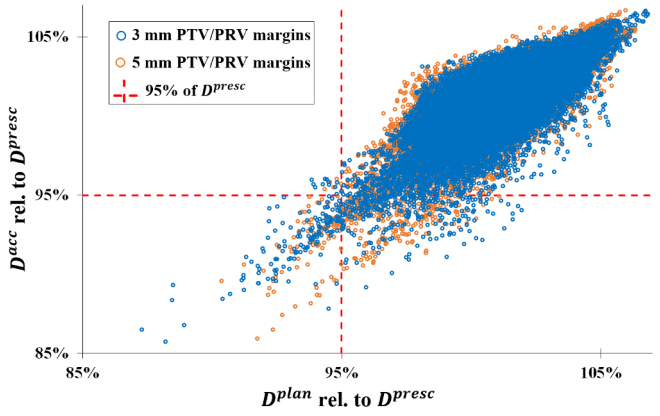

Fig. 3. Plot of individual voxels within the high-dose clinical target volumes (CTVs) of all patients when utilizing 3 or 5 mm planning target volume (PTV) and planning risk volume (PRV) margin plans. D^{plan} = planned dose. D^{acc} = accumulated dose. D^{presc} = prescribed dose.

by the analysis of the local target coverage near the skin. Fig. 4 shows that overall, a lower D^{plan}_{min} was obtained for the *local* CTVs that were closer to the skin. In addition, less superficial CTVs generally showed a slight increase in target coverage whereas the *local* CTVs more proximal to the skin displayed either preservation or a considerable drop in *local* coverage during treatment. These trends were very similar for both margin expansions and were independent of the magnitude of the contour change.

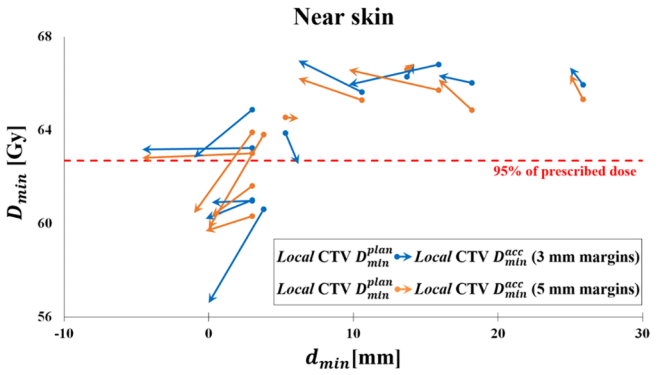

Fig. 4. Progression of the minimum planned dose D^{plan}_{min} to the minimum accumulated dose D^{acc}_{min} for local clinical target volumes (CTVs) near the skin for 3 and 5 mm planning target volume (PTV)/planning risk volume (PRV) margin plans. D^{plan}_{min} is plotted as a function of the minimum distance between the CTV and skin. D^{acc}_{min} is plotted as a function of the minimum distance between the CTV and skin, and the local shift of the skin at the end of treatment to indicate observed anatomical changes.

3.2. OARs

Application of reduced PTV/PRV margins had a beneficial impact on the dosimetry for OARs (Table 1). A significantly different $D^{plan}_{0.1cc}$ was achieved for the spinal cord (SC) PRV and brainstem (BS) PRV with 3 mm margin expansions. In addition, a compromise between target coverage and maximum dose to the BS PRV due to their proximity could be avoided for one patient by using 3 mm margin expansions, whereas a higher dose than the tolerance for the BS PRV had to be accepted to obtain sufficient target coverage both for the clinical plan and for the 5 mm plan in this study. More detail on the change in dosimetry of OARs during treatment for individual cases is provided in Supplementary Material F. A significantly different D^{plan}_{mean} could be obtained using 3 mm margin expansions for all salivary glands. The commonly used cut-off point in normal tissue complication probability (NTCP) models [32,33] stating that the PG D^{plan}_{mean} should be preferably less than 26 Gy was achieved in 8 and 14 cases (Supplementary Material A) for 5 and 3 mm margin expansions, respectively. The change in PG mean dose during treatment was generally less than 1 Gy and not significantly different for the two margin expansions (Fig. E.1; Supplementary Material F).

4. Discussion

The current study used DIR-facilitated dose accumulation to assess the actually delivered dose in the presence of anatomical changes, and the impact of a reduced PTV margin on the robustness of target coverage for anatomical changes. The CTV coverage $D^{acc}_{99\%}$ was found to be similar for both margin expansions and for only one case, this was less than 95% of the prescribed dose D^{presc} at the 95% level of confidence. However for many cases, the accumulated dose included a substantial volume of voxels receiving less than 95% D^{presc} independent of margin expansion. This predominantly occurred in the subdermal region.

Whether or not a PTV margin reduction is safe depends on many department-specific factors and can ultimately only be established by reviewing clinical results. Chen et al. [15,16] reported a 78% and 80% three-year LR control rate for the patient groups treated with 5 and 3 mm PTV margins, respectively ($p = 0.75$). Similarly, Navran et al. [17] reported that the two-year LR control rates equal to 79.2% and 79.9% for patients treated with 5 and 3 mm PTV margins, respectively, were not significantly different ($p = 1.0$). In contrast to the previous two groups, Franzese et al. [18] found a significant difference ($p = 0.045$) in LR control rates which were 87.8% and 72.6% for patients treated with 5 and 3 mm PTV margins at two-year follow-up,

respectively. Unfortunately, the above clinical results studies did not have a common approach to GTV to CTV margins, treatment adaptation, and treatment plan acceptance criteria. It is therefore not possible to conclude what caused the mixed clinical results and whether a PTV margin reduction is generally safe remains equivocal. The retrospective DIR-based dose accumulation studies by van Kranen et al. [19] and Wu et al [20] investigated the impact of anatomical changes to the dose delivery during modulated HNRT for different PTV margin expansions. Both studies used DVH metrics to assess the planned and delivered dose and, well aligned with the results of the current study, both studies reported a reduction in OAR dose with reduced margin expansions and a limited change in target coverage as indicated by DVH metrics. The study by van Kranen et al. [19] which used dose accumulation based on DIR of daily CBCT images reported a CTV $D_{99\%}^{acc}$ less than 95% of D^{presc} for only 1/19 and 2/19 cases for 5 and 3 mm PTV margin expansions, respectively. The study by Wu et al. [20] used dose accumulation based on weekly re-CTs included eleven patients. This study concluded that the coverage of the CTVs at the end of treatment was not affected by anatomical changes based on the ratio of multiple DVH metrics relative to the corresponding planning metrics. It should be noted that the current study and those by van Kranen et al. [19] and Wu et al. [20] may be restricted by limitations of DIR in the presence of mass and density changes [34–39]. The impact of this limitation is partially included in the dose accumulation uncertainty estimate that was used in the current study [27]. In addition, the current study and similar retrospective studies [19,20] only evaluated the plan robustness for anatomical changes during treatment. A full PTV margin estimate should include all geometrical uncertainties as sufficiently described in literature [5,10,11]. Due to the absence of a gold standard for delineation accuracy and limited knowledge on microscopic tumor spread for different tumor types [40–42], the only way to fully assess the validity of applied treatment margins is by pattern of failure studies or a review of clinical results as exemplified in refs [15–18] which must include consistent volume definitions [21,43]. However, we recommend that more comprehensive information is provided in review of clinical results studies including a voxel-based analysis of the actually delivered dose.

The initial analysis of target coverage based on DVH metrics in the current study suggested that 5 and 3 mm PTV margin plans have similar target coverage with only one 5 mm treatment plan where the HD-CTV target coverage was below the rejection criterion $D_{99\%}^{acc} < 95\%D^{presc}$ at the 95% level of confidence (Table 1). However, a full analysis of the dose delivered to each voxel (Table 2) highlighted potentially clinically significant underdosage in many cases both for 3 mm and 5 mm margin expansions. DVH metrics inherently lack spatial information regarding the dose distribution within a volume of interest [31] and commonly refer to percentages instead of absolute volumes. Specifically for larger target volumes, underdosage of the high- and intermediate-risk target volumes may not be detected by using DVH metrics as criterion. Therefore, a voxel-specific analysis of the entire target volume as is presented in the current study is preferred.

For the majority of cases with voxels receiving less than 95% D^{presc}, these voxels were located in the dermal region. Pattern of failure studies in literature that did explicitly document the locations of marginal locoregional recurrence (LRR) indicated that these occur relatively frequently in the subcutaneous/dermal region. Specifically, subcutaneous/dermal recurrences constituted 45% (4/9) [15], 60% (3/5) [44], 100% (1/1) [45] and 22% (2/9) [46] of the marginal LRRs in these reports. No dermal recurrences were observed for the patients included in the current study (median follow up 32 months, range 7–44 months). Further retrospective review of the study cases by the most senior clinician of our department involved in HNRT revealed that in some cases the observed underdosage of specific voxels in this study could potentially be clinically relevant. However, in most cases the CTV contour near the skin might have been slightly too generous with contour extension beyond the platysma and the observed underdosage of specific voxels in this study might not be clinically relevant for those cases. It should be noted that a slightly less generous CTV contour would also have resulted in a different treatment plan with likely one or more locations presenting a compromise in target coverage. As per the current departmental procedure, this study applied “virtual bolus” during plan optimization when CTVs extended into the dermal region [26] to moderate the fluence in the skin region and reduce the risk of severe skin toxicity. This approach commonly results in tight target coverage near the skin but is generally accepted by the treating clinician as compromise rather than using bolus on treatment unless the skin itself is at risk.

For 3D-conformal radiation treatments, the accuracy of the accumulated skin dose is limited by the uncertainty in the calculated dose in the buildup region [47]. However for VMAT treatments in this study, the dose to skin could be regarded as exit dose because the majority of dose to the skin was delivered through medial beam angles. Using the methodology previously developed for time-resolved point dose QC to assess the TPS calculated dose per control point [48], it could be demonstrated that ~80% of the dose delivered to 40 superficial HD-CTV points with $D^{acc} < 95\% D^{presc}$ was deposited at beam angles where the effective depth was larger than or equal to 4 mm. More detail on this analysis is provided in Supplementary Material G. In general, full scatter conditions can simply be achieved by immobilization devices such as radiation masks ‘behind’ the patient. Therefore, the exit dose follows the normal percentage depth dose curve and can be accurately calculated [47,49,50]. The accuracy of the skin dose calculation could also be limited by uncertainty in the Hounsfield units (HUs) of the most superficial voxels within the body contour [51]. Supplementary Material H details the results of planning simulations using an HU override equal to the average HU value ± 100 for these voxels. The HD-CTV doses were assessed for both HU values and the largest resulting 95% percentile range of the difference was ~1% D^{presc}. It is therefore reasonable to assume that any uncertainty in the HU of superficial regions has minimal impact on the observed values of HD-CTV D^{acc}, which were as low as ~85% D^{presc} (Fig. 3).

In the current study, loss in CTV coverage was very patient specific and appeared to be independent of margin expansion. Specifically for superficial HD-CTVs, the loss in *local* target coverage occurred more frequently in regions near the skin, but appeared not to be correlated with the magnitude of anatomical changes. In general, multiple mechanisms play a role in target coverage differences between planning and treatment. The interplay between local fluence, dose delivered per gantry angle, contribution of scatter and anatomical changes prohibited a clear identification of risk factors for individual patients that may be prone to a loss in target coverage during treatment. Nevertheless, it was clear that target coverage at treatment planning was an important factor considering that changes in patient anatomy on treatment are more likely to result in a decrease in target coverage when it was already marginal or compromised during the treatment preparation stage. It is recommended to assess target coverage using a voxel-based approach and not exclusively rely on DVH metrics. In principle this is not different from a slice-by-slice review of the 3D dose distribution before acceptance at treatment preparation by the treating radiation oncologist. However, manual review of the delivered dose after each fraction would be very laborious and automated processing of results using a voxel based analysis would be preferable for efficiency reasons.

In addition to increased sparing of salivary glands as described by many other studies [19,20,52], this study also highlighted the increased avoidance of the critical OARs with reduced PTV margins. As the minimum distance between the HD-CTV and BS decreased, a higher D_{min}^{plan} to the *local* PTV was generally achievable with 3 than with 5 mm margins (Fig. E.2a; Supplementary Material F). Comparably, as the minimum distance between the HD-CTV and BS decreased a lower D_{max}^{plan} to the *local* PRV was generally achievable with 3 mm margins (Fig. E.2c; Supplementary Material F). The compromise to the local BS PRV D_{max}^{plan} as required for the 5 mm margin plan for patient ten was not necessary

for the 3 mm plan.

In summary, a PTV/PRV margin reduction from 5 to 3 mm itself did not change the plan robustness for anatomical changes during treatment. However, a considerable loss in CTV coverage was observed for some patients irrespective of the margin expansion. Although this was very patient specific, it was specifically observed when target coverage at treatment planning was already tight. Patient-specific verification of dose delivery during treatment is therefore recommended, for instance using the DIR-facilitated dose accumulation analysis presented in the current study.

Declaration of Competing Interest

The authors declare that they have no known competing financial interests or personal relationships that could have appeared to influence the work reported in this paper.

Acknowledgements

We like to thank David Hamilton for reviewing and assessing the potential clinical impact of our dose accumulation results. NL received grants from the New Zealand Department of Internal Affairs (Lottery Health Research) and from Universities New Zealand (Edward and Isabel Kidson Scholarship).

Appendix A. Supplementary data

Supplementary data to this article can be found online at https://doi.org/10.1016/j.phro.2020.05.004.

References

[1] Mendenhall WM, Amdur RJ, Palta JR. Intensity-modulated radiotherapy in the standard management of head and neck cancer: promises and pitfalls. J Clin Oncol 2006;24:2618–23. https://doi.org/10.1200/JCO.2005.04.7225.
[2] Nutting CM, Morden JP, Harrington KJ, Urbano TG, Bhide SA, Clark C, et al. Parotid-sparing intensity modulated versus conventional radiotherapy in head and neck cancer (PARSPORT): a phase 3 multicentre randomised controlled trial. Lancet Oncol 2011;12:127–36. https://doi.org/10.1016/S1470-2045(10)70290-4.
[3] Pacholke HD, Amdur RJ, Morris CG, Li JG, Dempsey JF, Hinerman RW, et al. Late xerostomia after intensity-modulated radiation therapy versus conventional radiotherapy. Am J Clin Oncol Cancer Clin Trials 2005;28:351–8. https://doi.org/10.1097/01.coc.0000158826.88179.75.
[4] van Herk M. Different styles of image-guided radiotherapy. Semin Radiat Oncol 2007;17:258–67. https://doi.org/10.1016/j.semradonc.2007.07.003.
[5] Rasch C, Steenbakkers R, Van Herk M. Target definition in prostate, head, and neck. Semin Radiat Oncol 2005;15:136–45. https://doi.org/10.1016/j.semradonc.2005.01.005.
[6] International Commission on Radiation Units and Measurements. ICRU report 62: Prescribing, recording and reporting photon beam therapy (supplement to ICRU report 50); 1999.
[7] Suzuki M, Nishimura Y, Nakamatsu K, Okumura M, Hashiba H, Koike R, et al. Analysis of interfractional set-up errors and intrafractional organ motions during IMRT for head and neck tumors to define an appropriate planning target volume (PTV)- and planning organs at risk volume (PRV)-margins. Radiother Oncol 2006;78:283–90. https://doi.org/10.1016/j.radonc.2006.03.006.
[8] Manning MA, Wu Q, Cardinale RM, Mohan R, Lauve AD, Kavanagh BD, et al. The effect of setup uncertainty on normal tissue sparing with IMRT for head-and-neck cancer. Int J Radiat Oncol Biol Phys 2001;51:1400–9. https://doi.org/10.1016/S0360-3016(01)01740-0.
[9] Samuelsson A, Mercke C, Johansson K-A. Systematic set-up errors for IMRT in the head and neck region: effect on dose distribution. Radiother Oncol 2003;66:303–11.
[10] Van Herk M. Errors and Margins in Radiotherapy. Semin Radiat Oncol 2004;14:52–64. https://doi.org/10.1053/j.semradonc.2003.10.003.
[11] Van Herk M, Remeijer P, Rasch C, Lebesque JV. The probability of correct target dosage: Dose-population histograms for deriving treatment margins in radiotherapy. Int J Radiat Oncol Biol Phys 2000;47:1121–35. https://doi.org/10.1016/S0360-3016(00)00518-6.
[12] Barker JL, Garden AS, Ang KK, O'Daniel JC, Wang H, Court LE, et al. Quantification of volumetric and geometric changes occurring during fractionated radiotherapy for head-and-neck cancer using an integrated CT/linear accelerator system. Int J Radiat Oncol Biol Phys 2004;59:960–70. https://doi.org/10.1016/j.ijrobp.2003.12.024.
[13] Lowther NJ, Hamilton DA, Kim H, Evans JM, Marsh SH, Louwe RJW. Monitoring anatomical changes of individual patients using statistical process control during head-and-neck radiotherapy. Phys Imaging Radiat Oncol 2019;9:21–7. https://doi.org/10.1016/j.phro.2018.12.004.
[14] Brouwer CL, Steenbakkers RJHM, Langendijk JA, Sijtsema NM. Identifying patients who may benefit from adaptive radiotherapy: Does the literature on anatomic and dosimetric changes in head and neck organs at risk during radiotherapy provide information to help? Radiother Oncol 2015;115:285–94. https://doi.org/10.1016/j.radonc.2015.05.018.
[15] Chen AM, Yu Y, Daly ME, Farwell GD, Benedict SH, Purdy JA. Long-term experience with reduced planning target volume margins and intensity-modulated radiotherapy with daily image-guidance for head and neck cancer. Head Neck 2014;36:1766–72. https://doi.org/10.1002/hed.23532.
[16] Chen AM, Farwell DG, Luu Q, Donald PJ, Perks J, Purdy JA. Evaluation of the planning target volume in the treatment of head and neck cancer with intensity-modulated radiotherapy: What is the appropriate expansion margin in the setting of daily image guidance? Int J Radiat Oncol Biol Phys 2011;81:943–9. https://doi.org/10.1016/j.ijrobp.2010.07.017.
[17] Navran A, Heemsbergen W, Janssen T, Hamming-Vrieze O, Jonker M, Zuur C, et al. The impact of margin reduction on outcome and toxicity in head and neck cancer patients treated with image-guided volumetric modulated arc therapy (VMAT). Radiother Oncol 2018;130:25–31. https://doi.org/10.1016/j.radonc.2018.06.032.
[18] Franzese C, Fogliata A, Franceschini D, Navarria P, Cozzi L, Tomatis S, et al. Impact of hypofractionated schemes in radiotherapy for locally advanced head and neck cancer patients. Laryngoscope 2019:1–8. https://doi.org/10.1002/lary.28048.
[19] van Kranen S, Hamming-Vrieze O, Wolf AAL, Damen E, van Herk M, Sonke JJ. Head and neck margin reduction with adaptive radiation therapy: robustness of treatment plans against anatomy changes. Int J Radiat Oncol Biol Phys 2016;96:653–60. https://doi.org/10.1016/j.ijrobp.2016.07.011.
[20] Wu Q, Chi Y, Chen PY, Krauss DJ, Yan D, Martinez A. Adaptive replanning strategies accounting for shrinkage in head and neck IMRT. Int J Radiat Oncol Biol Phys 2009;75:924–32. https://doi.org/10.1016/j.ijrobp.2009.04.047.
[21] Grégoire V, Evans M, Le QT, Bourhis J, Budach V, Chen A, et al. Delineation of the primary tumour Clinical Target Volumes (CTV-P) in laryngeal, hypopharyngeal, oropharyngeal and oral cavity squamous cell carcinoma: AIRO, CACA, DAHANCA, EORTC, GEORCC, GORTEC, HKNPCSG, HNCIG, IAG-KHT, LPRHHT, NCIC CTG, NCRI. NRG Oncolog. Radiother Oncol 2018;126:3–24. https://doi.org/10.1016/j.radonc.2017.10.016.
[22] Grégoire V, Levendag P, Ang KK, Bernier J, Braaksma M, Budach V, et al. CT-based delineation of lymph node levels and related CTVs in the node-negative neck: DAHANCA, EORTC, GORTEC, NCIC, RTOG consensus guidelines. Radiother Oncol 2003;69:227–36. https://doi.org/10.1016/j.radonc.2003.09.011.
[23] Doornaert P, Verbakel WFAR, Bieker M, Slotman BJ, Senan S. RapidArc planning and delivery in patients with locally advanced head-and-neck cancer undergoing chemoradiotherapy. Int J Radiat Oncol Biol Phys 2011;79:429–35. https://doi.org/10.1016/j.ijrobp.2009.11.014.
[24] Verbakel W, Cuijpers JP, Hoffmans D, Bieker M, Slotman BJ, Senan S. Volumetric intensity-modulated arc therapy Vs. conventional IMRT in head-and-neck cancer: a comparative planning and dosimetric study. Int J Radiat Oncol Biol Phys 2009;74:252–9. https://doi.org/10.1016/j.ijrobp.2008.12.033.
[25] ICRU. ICRU Report 83 – Prescribing, Recording, and Reporting Photon Beam Therapy. vol. 10. 2010. https://doi.org/10.1093/jicru/ndq002.
[26] Thomas SJ, Hoole ACF. The effect of optimization on surface dose in intensity modulated radiotherapy (IMRT). Phys Med Biol 2004;49:4919–28. https://doi.org/10.1088/0031-9155/49/21/005.
[27] Lowther NJ, Marsh SH, Louwe RJW. Quantifying the dose accumulation uncertainty after deformable image registration in head-and-neck radiotherapy. Radiother Oncol 2020;143:117–25. https://doi.org/10.1016/j.radonc.2019.12.009.
[28] Kikinis R, Pieper SD, Vosburgh K. 3D Slicer: a platform for subject-specific image analysis, visualization, and clinical support. Intraoperative imaging image-guided Ther. New York, NY: Springer; 2014. p. 277–89.
[29] Pinter C, Lasso A, Wang A, Jaffray D, Fichtinger G. SlicerRT: radiation therapy research toolkit for 3D slicer. Med Phys 2012;39:6332–8. https://doi.org/10.1118/1.4754659.
[30] Teoh M, Clark CH, Wood K, Whitaker S, Nisbet A. Volumetric modulated arc therapy: a review of current literature and clinical use in practice. Br J Radiol 2011;84:967–96. https://doi.org/10.1259/bjr/22373346.
[31] Njeh CF, Parker BC. Evaluation of treatment plans using target and normal tissue DVHs is no longer appropriate. Med Phys 2015;42:2099–102. https://doi.org/10.1118/1.4903902.
[32] Eisbruch A, Ten Haken RK, Kim HM, Marsh LH, Ship JA. Dose, volume, and function relationships in parotid salivary glands following conformal and intensity-modulated irradiation of head and neck cancer. Int J Radiat Oncol Biol Phys 1999;45:577–87. https://doi.org/10.1016/S0360-3016(99)00247-3.
[33] Dijkema T, Raaijmakers CPJ, Ten Haken RK, Roesink JM, Braam PM, Houweling AC, et al. Parotid gland function after radiotherapy: the combined Michigan and Utrecht experience. Int J Radiat Oncol Biol Phys 2010;78:449–53. https://doi.org/10.1016/j.ijrobp.2009.07.1708.
[34] Yeo UJ, Taylor ML, Supple JR, Smith RL, Dunn L, Kron T, et al. Is it sensible to "deform" dose 3D experimental validation of dose-warping. Med Phys 2012;39:5065–72. https://doi.org/10.1118/1.4736534.
[35] Schultheiss TE, Tome WA, Orton CG. Point/counterpoint: it is not appropriate to "deform" dose along with deformable image registration in adaptive radiotherapy. Med Phys 2012;39:6531–3. https://doi.org/10.1118/1.4722968.
[36] Zhong H, Chetty IJ. Caution must be exercised when performing deformable dose accumulation for tumors undergoing mass changes during fractionated radiation therapy. Int J Radiat Oncol Biol Phys 2017;97:182–3. https://doi.org/10.1016/j.ijrobp.2016.09.012.
[37] Hugo GD, Dial C, Siebers JV. In regard to Zhong and Chetty. Int J Radiat Oncol

2017;99:1308–10. https://doi.org/10.1016/j.ijrobp.2017.08.047.
[38] Taylor ML, Siva S, Franich RD, Yeo UJ, Pham D, Supple J, et al. Comment on “It is not appropriate to ‘deform’ dose along with deformable image registration in adaptive radiotherapy” [Med. Phys. 39, 6531-6533 (2012)]. Med Phys 2013;40:017101. https://doi.org/10.1118/1.4771962.
[39] Chetty IJ, Rosu-Bubulac M. Deformable registration for dose accumulation. Semin Radiat Oncol 2019;29:198–208. https://doi.org/10.1016/j.semradonc.2019.02.002.
[40] Campbell S, Poon I, Markel D, Vena D, Higgins K, Enepekides D, et al. Evaluation of microscopic disease in oral tongue cancer using whole-mount histopathologic techniques: Implications for the management of head-and-neck cancers. Int J Radiat Oncol Biol Phys 2012;82:574–81. https://doi.org/10.1016/j.ijrobp.2010.09.038.
[41] Apisarnthanarax S, Elliott DD, El-Naggar AK, Asper JA, Blanco A, Ang KK, et al. Determining optimal clinical target volume margins in head-and-neck cancer based on microscopic extracapsular extension of metastatic neck nodes. Int J Radiat Oncol Biol Phys 2006;64:678–83. https://doi.org/10.1016/j.ijrobp.2005.08.020.
[42] Caldas-Magalhaes J, Kooij N, Ligtenberg H, Jager EA, Schakel T, Kasperts N, et al. The accuracy of target delineation in laryngeal and hypopharyngeal cancer. Acta Oncol (Madr) 2015:1–7. https://doi.org/10.3109/0284186X.2015.1006401.
[43] Brouwer CL, Steenbakkers RJHM, Bourhis J, Budach W, Grau C, Grégoire V, et al. CT-based delineation of organs at risk in the head and neck region Oncology and TROG consensus guidelines. Radiother Oncol 2015;117:1–291.
[44] Ooishi M, Motegi A, Kawashima M, Arahira S, Zenda S, Nakamura N, et al. Patterns of failure after postoperative intensity-modulated radiotherapy for locally advanced and recurrent head and neck cancer. Jpn J Clin Oncol 2016;46:919–27. https://doi.org/10.1093/jjco/hyw095.
[45] Bayman E, Prestwich RJD, Speight R, Aspin L, Garratt L, Wilson S, et al. Patterns of failure after intensity-modulated radiotherapy in head and neck squamous cell carcinoma using compartmental clinical target volume delineation. Clin Oncol 2014;26:636–42. https://doi.org/10.1016/j.clon.2014.05.001.
[46] Shakam A, Scrimger R, Liu D, Mohamed M, Parliament M, Field GC, et al. Dose-volume analysis of locoregional recurrences in head and neck IMRT, as determined by deformable registration: a prospective multi-institutional trial. Radiother Oncol 2011;99:101–7. https://doi.org/10.1016/j.radonc.2011.05.008.
[47] Kry S, Smith S, Weathers R, Stovall M. Skin dose during radiotherapy: a summary and general estimation technique. J Appl Clin Med Phys 2012;13:20–34.
[48] Louwe RJW, Wendling M, Monshouwer R, Satherley T, Day RA, Greig L. Time-resolved dosimetry using a pinpoint ionization chamber as quality assurance for IMRT and VMAT. Med Phys 2015;42:1625–39. https://doi.org/10.1118/1.4914395.
[49] Purdy JA. Buildup/surface dose and exit dose measurements for a 6-MV linear accelerator. Med Phys 1986;13:259–62.
[50] Klein E, Purdy JA. Entrance and exit dose regions for a clinac-2100c. Int J Radiat Oncol Biol Phys 1993;27:429–35.
[51] Branchini M, Broggi S, Dell’Oca I, Cattaneo GM, Calandrino R, Di Muzio NG, et al. Skin dose calculation during radiotherapy of head and neck cancer using deformable image registration of planning and mega-voltage computed tomography scans. Phys Imaging Radiat Oncol 2018;8:44–50. https://doi.org/10.1016/j.phro.2018.11.008.
[52] O’Daniel JC, Garden AS, Schwartz DL, Wang H, Ang KK, Ahamad A, et al. Parotid gland dose in intensity-modulated radiotherapy for head and neck cancer: is what you plan what you get? Int J Radiat Oncol Biol Phys 2007;69:1290–6. https://doi.org/10.1016/j.ijrobp.2007.07.2345.